Synthesis and evaluation of an agrocin 84 toxic moiety (TM84) analogue as a malarial threonyl tRNA synthetase inhibitor

Synthesis and Evaluation of a Agrocin 84 Toxic Moiety (TM84) analogue as a Malarial Threonyl tRNA Synthetase Inhibitor

Jhon Alexander Rodriguez Buitrago,[a] Gundars Leitis,[a] Iveta Kaņepe-Lapsa,[a] Anastasija Rudnickiha,[a] Emilio Parisini[a,b]* and Aigars Jirgensons[a]*

An analogue of a toxic moiety (TM84) of natural product Agrocin 84 containing threonine amide instead of 2,3-dihydroxy-4-methylpentanamide was prepared and evaluated as putative *Plasmodium falciparum* threonyl t-RNA synthetase (PfThrRS) inhibitor. This TM84 analogue features submicromolar inhibitory potency (IC_{50} = 440 nM) comparable to that of borrelidin (IC_{50} = 43 nM) and therefore complements chemotypes known to inhibit malarial PfThrRS, which are currently limited to borrelidin and its analogues. The crystal structure of the inhibitor in complex with the *E. Coli* homologue enzyme (EcThrRS) was obtained, revealing crucial ligand-protein interactions that will pave the way to the design of novel ThrRS inhibitors.

Introduction

Malaria is a vector born disease caused by plasmodium parasites, which are transmitted by mosquitoes. The disease impacts on half of the world's population living in tropical and sub-tropical areas, causing around 600 thousand annual deaths.[1] The constant spread of drug-resistant plasmodium parasites[2,3] highlights the need for the discovery of new drugs with unexploited mode of action. Aminoacyl t-RNA synthetases (aaRS) are a group of enzymes that contribute to protein biosynthesis by charging t-RNA with the cognate amino acid via a two-step enzymatic reaction that involves the formation of aminoacyladenosine (compound **1**, Figure 1) as a reactive intermediate.

Aminoacyl t-RNA synthetases have received considerable attention as possible targets for the development of anti-infective agents,[4-11] including antimalarial drugs.[12-14] Among them, threonyl t-RNA synthethase (ThrRS) has been proved to be targeted by the natural product borrelidin (compound **2**, Figure 1) and its analogues. Indeed, these compounds have been shown to feature very potent anti-malarial activity in both infected cell assays and in mice infection models.[15-17] To date, while several classes of bacterial ThrRS inhibitors have been developed,[18-22] known *Plasmodium falciparum* ThrRS (PfThrRS) inhibitors are still limited to borrelidin and its analogues. Hence, to expand the range of putative malarial ThrRS inhibitors, we searched for alternative chemotypes. TM-84 (compound **3a**, Figure 1), a toxic moiety of the natural product Agrocin 84 (compound **3b**, Figure 1), is known to be a leucyl t-RNA synthetase inhibitor.[23,24] While **3a** can be considered as a structural mimic of aminoacyladenosine intermediate **1**, it contains deoxyarabinose instead of ribose and a 2,3-dihydroxy-4-methylpentanamide moiety linked to the nucleoside *via* a non-hydrolyzable phosphoramide bond. Interestingly, **3a** binds weakly to the active site of the enzyme in the absence of t-RNA. The formation of a hydrogen bond between **3a** and the 3'-terminal adenosine of the t-RNA molecule is needed to stabilize the ternary complex, resulting in the deactivated enzyme.

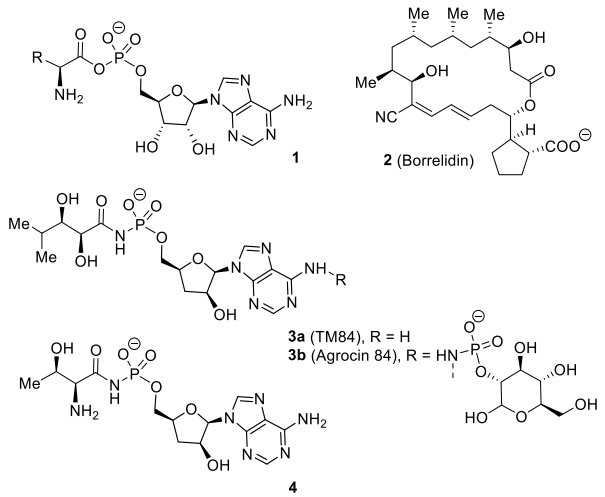

Figure 1. An intermediate of the enzymatic reaction of aaRS, aminoacyladenosine **1** and aaRS inhibitors: **2** (borrelidin); **3a** (TM84); **3b** (Agrocin 84) and **4**, the analogue of TM84

We aimed to use **3a** as a scaffold to develop PfThrRS inhibitor **4** (Figure 1) by replacing the dihydroxyacyl substructure in **3a** with threonine.

Results and discussion

Synthesis of compound 4

A deoxyarabinose containing nucleoside building block **11** for the synthesis of target compound **4** was prepared according to Scheme 1. The synthesis started from adenosine (**5**) which was transformed

to nucleoside **8** by using the procedures described in literature.[25] The procedures involved selective *O*-pivaloyl protection to give dipivaloyl derivative **6** which was *O*-mesylated to give an intermediate **7**. The reduction of compound **7** resulted in 3'O-deoxygenation and inversion of stereocenter at 2'-position provided deoxyarabinose nucleoside **8** *via* an *in situ* generated 3'-deoxy-2'-keto intermediate. Nucleoside **8** was *O*-TBS protected at the primary alcohol to give intermediate **9**, which was *O*-acylated at the secondary alcohol to give acetate **10**. The cleavage of the TBS group provided the desired building block **11**.

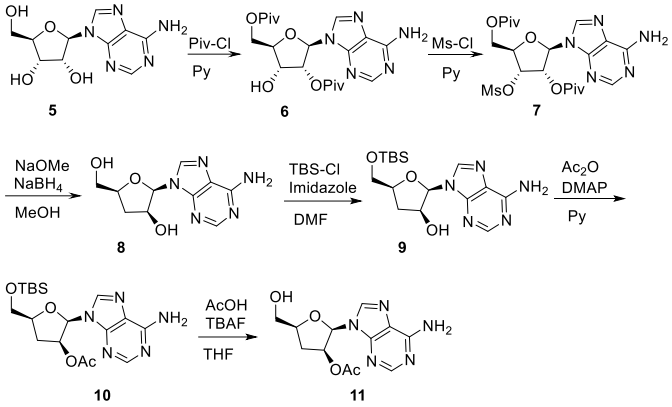

Scheme 1. Synthesis of nucleoside building block **11**

To complete the synthesis of target compound **4**, protected threonine **12** was first transformed to an amide **13** (Scheme 2).

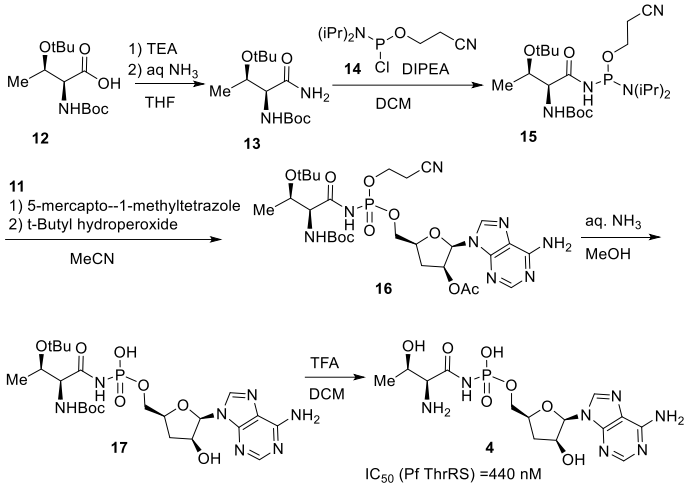

Scheme 2. Synthesis of inhibitor **4** by attachment of threonine to adenosine *via* phosphoramide linkage.

This was further subjected to the reaction with *O*-cyanoethylchlorophosphoramidite **14**. The resulting intermediate **15** was coupled to a building block **11**, the protected phosphordiamidite was oxidized to phosphoramide **16**. Cleavage of cyanoethyl protecting group from phosphoramide and acetyl group from 2'-hydroxy group provided an intermediate **17** which was subjected to the deprotection of threonine part to give the final product **4**.

***In vitro* PfThrRS inhibitory potency of compound 4**

Compound **4** was tested for its ability to inhibit PfThrRS in a biochemical assay based on the measurement of ATP consumption in an enzymatic reaction.[18] The inhibitory potency of compound **4** was found to be in the nanomolar range (IC_{50} = 440 ± 60 nM), i.e. 10-fold lower than that we have determined for borrelidin (**2**) (IC_{50} = 43 ± 5nM) (Supplementary Figures S14a-c).

Affinity of compound 4 to EcThrRS

The dissociation constant (K_D) of compound **4** bound to EcThrRS was assessed by isothermal titration calorimetry (ITC) and was found to be equal to 121 ± 36 nM (Supplementary Figure S15).

Crystal structure of *E. coli* threonyl-tRNA synthetase in complex with inhibitor 4

The *E. coli* threonyl t-RNA synthetase (EcThrRS) dimer (PDB ID: 1NYQ) exhibits a high degree of structural similarity with its *Plasmodium falciparum* analogue (AlphaFold model ID:Q8IIA4 (Pf3D7)) and with the human threonyl t-RNA synthetase (PDB ID: 4P3N). It also shares with them a high degree of sequence similarity (53.2 and 62.4%, respectively).

EcThrRS is a modular protein comprising four distinct structural domains. The dimeric core consists mainly of the catalytic and *C*-terminal anticodon binding domains, while the two N-terminal domains of each monomer protrude from the core. The dimer interface is mainly formed by a class II–conserved motif 1 (residues 281 to 298) and by two short strands located before and after the motif. The *N*-terminal domains lie on opposite sides of the dimeric core and give the molecule an elongated shape. The catalytic module (residues 243–534) is built upon six antiparallel strands surrounded by three helices. The *C*-terminal domain (residues 535–642), which recognizes the anticodon bases, is a mixed a/b domain made of four antiparallel and one parallel β-strand surrounded by three α–helices. The *N*-terminal region (residues 1-224) is attached to the catalytic core through a linker helix (residues 225–242). This region is largely conserved in prokaryotes and eukaryotes, but is significantly different in the archaeal and yeast mitochondrial enzymes. All cytoplasmic ThrRS enzymes in eukaryotes have an additional extension of about 65 residues that has never been structurally characterized and may correspond to an additional structural domain. In the active site, the zinc ion is directly involved in the recognition of inhibitor **4**, forming a penta-coordinate intermediate with both the amino group and the side chain hydroxyl adjacent to the AMP-binding pocket (Figure 2). The Zn-coordinating ligands include His144, His270, and Cys93, with a water molecule completing the tetrahedral coordination of the ion. The overall pattern of interactions is illustrated in Figure 2.

ARTICLE

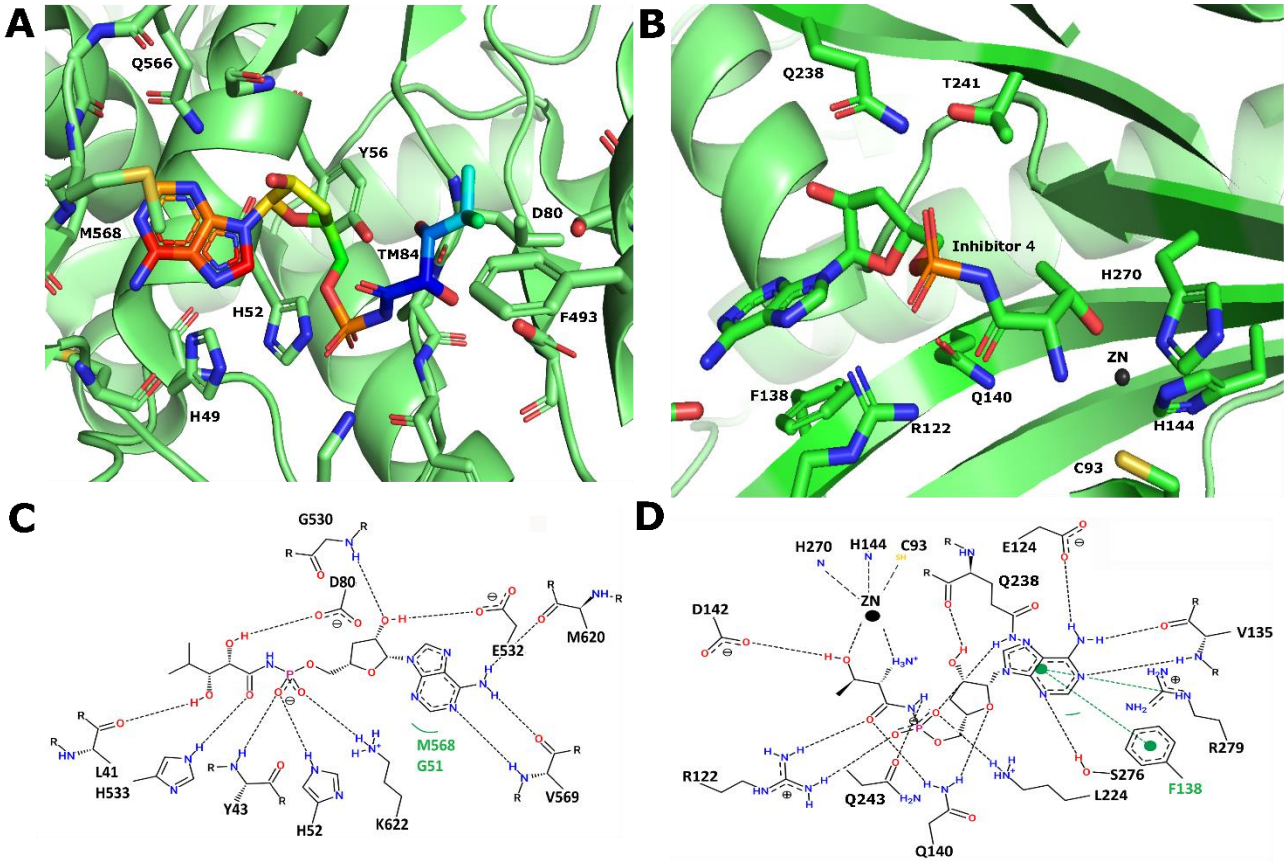

Figure 2. Binding mode comparison between *Ec*LeuRS bound to TM84 and *Ec*ThrRS bound to inhibitor 4. A,B The active site of the EcLeuRS with **3a** (TM84) and EcThrRS with inhibitor **4** in blue color. Inset: View of the active site showing the interactions with the zinc ion. The class-specific motifs 2 and 3 are colored red and green, respectively. The zinc ion and water molecule are represented as pink and cyan spheres. **C,D** The interaction network of the EcLeuRS with **3a** (TM84) and *Ec*ThrRS with inhibitor **4**.

Binding mode comparison between *Ec*LeuRS- TM84 and *Ec*ThrRS-inhibitor

Owing to their 11% sequence identity and low structural similarity, a superposition of the full length crystal structure of *E. coli* leucyl-tRNA synthetase (EcLeuRS) and *E. coli* threonyl-tRNA synthetase (EcThrRS) in complex with ligand **3a** and inhibitor **4**, respectively (PDB codes 3ZGZ and 8OU8, respectively) is not possible. However, a comparison of these two structures reveals several significant differences (Figures 2A,B). One of the main differences is that in the active site of EcThrRS there is a zinc ion that binds the threonine moiety of inhibitor **4** (Figure 2B). In addition to Zn coordination, the threonine hydroxyl group forms a hydrogen bond with Asp142 of EcThrRS. In the case of EcLeuRS, the zinc ion is absent and the dihydroxy moiety of **3a** (TM84) is stabilized by interactions with the amino acids Asp80, Phe493 and His537 (Figure 2A). This difference highlights the importance of the zinc ion as a unique feature for threonine recognition by ThrRS. Notably, inhibitor **4** is located in a compact conformation in the binding pocket of EcThrRS, differing from the extended conformation of **3a** (TM84) in the pocket of the EcLeuRS. The negatively charged acylphosphoramide moiety of **3a** (TM84) forms electrostatic interactions with His52 and Lys622 as well as hydrogen bonds with His533 and Tyr43 (Figure 2C). The insertion of positively charged Lys622 into the active site is electrostatically favored by the presence of the charged N-acyl phosphate group, while His52 makes an interaction with the other non-bridging oxygen of the phosphate moiety of TM84 (Figure 2C). The acylphosphoramide moiety of inhibitor **4** forms electrostatic interactions with Arg122, Lys224 and Gln238 (Figure 2B,D) as well as a water-mediated hydrogen bonding interaction with Tyr221. Whereas the hydroxyl group of the 3-deoxyarabinose moiety of **3a** (TM84) acts both as a hydrogen bond donor and acceptor by interacting with Gly530 and Glu532 (Figure 2C), the hydroxyl group of deoxyarabinose of inhibitor **4** is involved only as a hydrogen bond donor with Gln238 (Figure 2D). However, the oxygen of the tetrahydrofuran moiety of inhibitor **4** forms a hydrogen bonding interaction with Gln140. The adenosine moiety of **3a** (TM84) is

stabilized by interactions with the amino acids Gly51, Glu532, Gln566, Met568, Val569 and Met620 (Figure 2C). In the case of the inhibitor **4**, the adenosine moiety interacts with the amino acids Glu124, Gln238, Val135, Arg279, Phe138 and Ser276 (Figure 2D). Taken together, these structural observations indicate that inhibitor **4** occupies the ThrRS active site cavity that joins the two substrate-binding pockets for L-Thr and ATP and effectively excludes substrate (aminoacyl intermediate **1**) binding to ThrRS (Figure 2).

Experimental

Synthesis description

*(2R,3S,5S)-2-(6-Amino-9H-purin-9-yl)-5-(hydroxymethyl)tetrahydro-furan-3-ol (**8**).* Pivaloyl chloride (6.94 mL, 56.7 mmol) was added to a stirred suspension of adenosine (**5**) (5.0 g, 18.7 mmol) in dry pyridine (50 mL) at -15°C. The mixture was stirred first at this temperature for 1.5 h and then at 0°C for 2 h. Methanesulphonyl chloride (4.35 mL, 56.1 mmol) was added to the solution of pivaloyl derivative **6**and the mixture was stirred at room temperature for 3 h. The mixture was cooled in an ice bath then, ice water was added, and the mixture was extracted with diethyl ether containing a small amount of chloroform. The organic phase was washed once with aqueous sodium hydrogen carbonate and twice with water, dried over Na_2SO_4 and concentrated by evaporation *in vacuo*. Pyridine was removed by repeated co-evaporation with toluene. The crude methanesulphonate**7** was dissolved in MeOH (150 mL). To the solution was added 5.4 M NaOMe (27.71 mL, 149.7 mmol) and $NaBH_4$, (2.55 g, 67.4 mmol) at -15°C. The mixture was stirred first at room temperature for 14 h and then at 50°C for 5 h. The reaction mixture was cooled to room temperature and acetone was added. The resulting mixture was neutralized with concentrated aqueous hydrochloric acid and evaporated under reduced pressure. The remaining water was removed by repeated co-evaporation with ethanol. The residue was suspended in a mixture $CHCl_3$-MeOH and separated by silica gel column chromatography eluting with $CHCl_3$-MeOH (8: 1). Elution with the same solvent system (8: 1 to 5 : 1) gave product (2.2 g, 47%). The product **8** was recrystallized from MeOH (1.57 g, 33%). m.p. 192-193°C (dec.), (lit. 195-196°C). Elemental Analysis calcd.: C, 47.81; H, 5.22; N, 27.88; found: C, 47.76; H, 5.26; N, 27.78; $[\alpha]_D$=-24.3°(c=1, DMF) (lit. -24.3°, c=1.1, DMF);^{1}H NMR (400 MHz, DMSO-d_6) δ 8.29 (s, 1H), 8.13 (s, 1H), 7.23 (s, 2H), 6.15 (d, J = 5.4 Hz, 1H), 5.40 (d, J = 5.6 Hz, 1H), 5.15 (s, 1H), 4.57 – 4.44 (m, 1H), 4.15 – 4.03 (m, 1H), 3.71 – 3.53 (m, 2H), 2.37 – 2.22 (m, 1H), 2.09 – 1.96(m, 1H). ^{13}C NMR (400 MHz, DMSO-d_6) δ155.89, 152.32, 149.58, 140.14, 118.25, 84.42, 77.94, 70.21, 62.67, 33.86.

*(2R,3S,5S)-2-(6-Amino-9H-purin-9-yl)-5-(((tert-butyldimethylsilyl)oxy)methyl)tetrahydrofuran-3-ol (**9**).*TBS-Cl (1.08 g, 7.2 mmol) and imidazole (0.51 g, 7.5 mmol) was added to a solution of deoxyadenine **8** (1.5 g, 6.0 mmol) in DMF (20 mL) at 0°C, after stirring overnight H_2O (100 mL) was added, and the products were extracted with EtOAc (2 x 100 mL). The extracts were washed twice with brine, dried over Na_2SO_4 and concentrated *in vacuo*. Product **9** was used for the next step without purification. ^{1}H NMR (400 MHz, methanol-d_4) δ 10.05 (s, 1H), 9.75 (s, 1H), 7.79 (d, J = 5.2 Hz, 1H), 6.22 (ddd, J = 7.6, 6.6, 5.2 Hz, 1H), 5.81 (ddt, J = 8.5, 6.7, 3.3 Hz, 1H), 5.56 (dd, J = 11.4, 3.1 Hz, 1H), 5.40 (dd, J = 11.4, 3.6 Hz, 1H), 3.92 (dt, J = 13.1, 6.7 Hz, 1H), 3.74 (ddd, J = 13.0, 8.5, 7.6 Hz, 1H), 2.52 (s, 9H), 1.70 (d, J = 2.0 Hz, 6H). ^{13}C NMR (101 MHz, methanol-d_4) δ 157.18, 153.62, 150.62, 141.91, 119.67, 86.77, 79.65, 72.48, 65.48, 49.00, 34.04, 26.49, 19.38, -5.29.

(2R,3S,5S)-2-(6-Amino-9H-purin-9-yl)-5-(((tert-butyldimethylsilyl)oxy)methyl)tetrahydrofuran-3-yl acetate (**10**). The crude TBS-deoxyadenine derivative **9** (2.18 g, 6.00 mmol) was co-evaporated twice with dry pyridine. The residue was dissolved in pyridine and to this a solution Ac_2O (0.62 mL, 6.6 mmol) and DMAP (37 mg, 0.30 mmol) was added. After stirring overnight saturated Na_2CO_3 (100 mL) was added and the mixture was extracted with EtOAc(2 x 100mL). The combined organic phase were washed with brine, dried over Na_2SO_4 and concentrated *in vacuo*. Purification was performed by column chromatography on a silica gel eluting with hexanes/EtOAc 1:1 to 0:1 to provide product **10** (1.56 g, 64%) as crystalline material. m.p. 156-157. $[\alpha]_D$=-0.58° (c=1, MeOH). ^{1}H NMR (400 MHz, Methanol-d_4) δ 10.04 (s, 1H), 9.75 (s, 1H), 7.97 (d, J = 5.7 Hz, 1H), 7.28-7.20 (m, 1H), 5.90-5.82 (m, 1H), 5.61 (dd, J = 11.5, 3.2 Hz, 1H), 5.45 (dd, J = 11.5, 3.7 Hz, 1H), 4.08-3.98 (m, 1H), 3.95-3.84 (m, 1H), 3.24 (s, 3H), 2.53 (s, 9H), 1.71 (s, 6H).^{13}CNMR (101 MHz, Methanol-d_4) δ 170.90, 157.28, 153.89, 150.47, 141.32, 119.68, 84.75, 79.66, 74.06, 64.82, 31.06, 26.48, 26.19, 20.21, 19.37, -5.23, -5.27.HRMS-ESI (m/z) calcd. for $C_{18}H_{30}N_5O_4Si[M+H]^+$ 408.2067. Found 408.2078.

(2R,3S,5S)-2-(6-Amino-9H-purin-9-yl)-5-(hydroxymethyl)tetrahydrofuran-3-yl acetate (**11**). TBAF*3H_2O (1.62 g, 4.98 mmol) and AcOH (0.29 mL, 4.98 mmol) was added to a solution of deoxyadenine derivative **10** (1.56 g, 3.83 mmol) in THF (100 mL) and the mixture was stirred overnight. The mixture was evaporated on a silica gel and purified on a silica gel column, eluting with EtOAc/MeOH containing 5% of TEA. Collection and evaporation of pure fractions gave product **11** (570 mg, 51%) as crystalline material. m.p. 187-189. $[\alpha]_D$=-33.0° (DMSO-d_6). ^{1}H NMR (400 MHz, DMSO-d_6) δ 8.33 (s, 1H), 8.13 (s, 1H), 7.26 (s, 2H), 6.36 (d, *J* = 5.6 Hz, 1H), 5.55 (td, *J* = 7.5, 5.6 Hz, 1H), 5.11 (t, *J* = 5.6 Hz, 1H), 4.17 (dddd, *J* = 8.6, 6.4, 4.6, 3.7 Hz, 1H), 3.76 – 3.58 (m, 2H), 2.48 – 2.41 (m, 1H), 2.22 (ddd, *J* = 12.9, 9.0, 7.8 Hz, 1H), 1.67 (s, 3H).^{13}C NMR (101 MHz, DMSO-d_6) δ 169.05, 155.92, 152.56, 149.29, 139.52, 118.21, 82.54, 77.95, 72.27, 62.17, 39.52, 30.62, 20.11. HRMS-ESI (m/z) calcd. for $C_{12}H_{16}N_5O_4$ $[M+H]^+$ 294.1202. Found 294.1205

tert-Butyl ((2S,3R)-1-amino-3-(tert-butoxy)-1-oxobutan-2-yl)carbamate (**13**). To an ice cooled solution of protected threonine **12** (1.61 g, 5.85 mmol) in dry THF (20 mL), TEA (1.79 mL, 12.86 mmol) and ethylchloroformate (0.84 mL, 8.77 mmol) was added. White thick suspension was formed. The mixture was stirred for 20 min at room temperature and cooled again in an Ice bath. To this, 25% aqueous ammonia solution (20 mL) was added to the mixture was warmed up to room temperature in 30 min. Then saturated $NaHCO_3$ (100 mL) was added and the mixture was extracted with EtOAc (2x 100mL). The extracts were washed with brine, dried over Na_2SO_4 and concentrated *in vacuo*. ThE crude product was purified on a silica-gel column, eluting with hexanes/EtOAc 4:1, providing amide **13** (1.21 g, 75%) as crystalline material. m.p. 101-103. $[\alpha]_D$= 40.6° (MeOH). ^{1}H

NMR (400 MHz, chloroform-d) δ 6.94 (s, 1H), 5.71 – 5.50 (m, 1H), 5.43 (s, 1H), 4.19 – 4.00 (m, 2H), 1.45 (s, 10H), 1.27 (s, 10H), 1.07 (d, J = 6.2 Hz, 3H). ^{13}C NMR (101 MHz, $CDCl_3$) δ 172.38, 155.63, 79.68, 75.40, 66.79, 61.12, 58.46, 28.38, 17.17, 14.64. HRMS-ESI (m/z) calcd. for $C_{13}H_{26}N_2O_4Na$ $[M+Na]^+$ 297.1790. Found 297.1805

tert-Butyl((2S,3R)-3-(tert-butoxy)-1-(((2-cyanoethoxy)(diisopropylamino)phosphaneyl)amino)-1-oxobutan-2-yl)carbamate (**15**). To a solution of protected threonine amide **13** (300 mg, 1.01 mmol) in dry DCM (4 mL), DIPEA (0.57 mL, 3.28 mmol) and 2-cyanoethyl-diisopropyl-chlorophosphoramidite (**14**) (0.49 mL, 2.19 mmol) was added. The reaction mixture was stirred for 1h at room temperature and was diluted with $CHCl_3$(100 mL). An organic phase was washed with 1 M NaHCO and dried over Na_2SO_4. The extract was concentrated *in vacuo* and the crude product was purified on a silica gel column eluting with hexanes/EtOAc 4:1 to give carbamate **15** (480 mg, 92%). ^{1}H NMR (300 MHz, chloroform-d) δ 5.62 (s, 1H), 4.17 – 4.03 (m, 2H), 3.91 (dddt, J = 8.5, 6.8, 5.5, 2.8 Hz, 2H), 3.56 (dqd, J = 13.5, 6.8, 3.4 Hz, 2H), 2.63 (td, J = 6.3, 2.6 Hz, ^{13}C NMR (101 MHz, CDCl3) δ 172.88, 172.76, 172.47, 172.36, 171.17, 155.55, 117.55, 79.60, 77.16, 75.49, 67.16, 67.06, 60.45, 60.35, 60.23, 60.07, 59.97, 59.36, 59.05, 44.84, 44.71, 28.43, 24.59, 24.52, 24.45, 24.38, 21.13, 20.54, 20.46, 17.51, 17.09, 14.292H), 1.44 (s, 9H), 1.35– 1.13 (m, 21H), 1.07 (dd, J = 6.5, 3.9 Hz, 3H). HRMS-ESI (m/z) calcd. for $C_{22}H_{43}N_4O_6NaP$ $[M+O+Na]^+$ 513.2818. Found 513.2823

(2R,3S,5S)-2-(6-amino-9H-purin-9-yl)-5-(((((2S,3R)-3-(tert-butoxy)-2-((tert-butoxycarbonyl)amino)butanamido)(2-cyanoethoxy) phosphoryl)oxy)methyl)tetrahydrofuran-3-yl acetate **16**). (Carbamate **15** (324 mg, 0.68 mmol) and 5-mercapto-1-methyltetrazole (475 mg, 4.01 mmol) was added to a suspension of deoxyadenosine derivative **11** (200 mg, 0.68 mmol) in MeCN (20 mL). The mixture was stirred for 2 h at room temperature and to this t-BuOOH (0.25 mL, 1.36 mmol) was added. After stirring for 20 min at room temperature, saturated aqueous $NaHCO_3$ (50 mL) was added and the mixture was extracted with DCM (2 x 50mL). The combined organic phase was dried over Na_2SO_4 and concentrated *in vacuo*. The crude product was purified on a silica-gel column eluting with DCM containing MeOH 5-20% to give protected deoxyadenosine-threonine conjugate **16** (190 mg, 40%). ^{1}H NMR (400 MHz, Methanol-d4) δ 8.38 (d, J = 12.9 Hz, 1H), 8.21 (s, 1H), 6.48 (dd, J = 5.0, 1.0 Hz, 1H), 5.59 (dtd, J = 6.6, 5.5, 1.3 Hz, 1H), 4.58 – 4.47 (m, 2H), 4.36 (qt, J = 6.0, 1.7 Hz, 2H), 4.18 – 4.03 (m, 2H), 2.89 (ddd, J = 11.0, 5.5, 1.0 Hz, 2H), 2.70 (ddt, J = 13.6, 9.7, 6.8 Hz, 1H), 2.33 (tdd, J = 10.2, 8.8, 5.7 Hz, 1H), 1.79 (d, J = 5.2 Hz, 3H), 1.45 (d, J = 3.9 Hz, 9H), 1.24 – 1.06 (m, 12H).^{13}C NMR (101 MHz, Methanol-d4) δ 174.93, 170.84, 157.80, 157.25, 153.88, 150.47, 141.78, 119.68, 118.38, 85.92, 85.79, 81.01, 77.24, 75.92, 73.61, 73.55, 70.29, 70.02, 68.53, 64.21, 61.96, 61.86, 49.00, 32.85, 32.79, 28.67, 20.31, 20.15, 20.06. HRMS-ESI (m/z) calcd. for $C_{28}H_{44}N_8O_{10}P$ $[M+H]^+$ 683.2918. Found 683.2927

(2R,3S,5S)-2-(6-Amino-9H-purin-9-yl)-5-(((((2S,3R)-3-(tert-butoxy)-2-((tert-butoxycarbonyl)amino)butanamido)(hydroxy)phosphoryl)oxy) methyl)tetrahydrofuran-3-yl acetate (**17**). To a solution of protected deoxyadenosine-threonine conjugate **16** (190 mg, 0.26 mmol) in MeOH (30 mL) 25 % aqueous NH_3 (15 mL, 52.00 mmol) was added. The reaction mixture was stirred for 24 h and evaporated. The residue was applied to a silica-gel column eluating with EtOAc containing TEA 5% and MeOH 20-50% to give a product **17** containing TEA acetate. The product was placed in the ^{1}H NMR (400 MHz, methanol-d_4) δ 8.45 (s, 1H), 8.19 (s, 1H), 6.24 (d, J = 4.8 Hz, 1H), 4.64 – 4.52 (m, 1H), 4.42 – 4.30 (m, 1H), 4.18 (dd, J = 6.7, 4.9 Hz, 2H), 4.08 (d, J = 3.0 Hz, 2H), 2.48 (ddd, J = 13.6, 7.4, 6.4 Hz, 1H), 2.21 – 2.09 (m, 1H), 1.45 (s, 9H), 1.23 (s, 9H), 1.10 (d, J = 6.2 Hz, 3H). HRMS-ESI (m/z) calcd. for $C_{23}H_{39}N_7O_9P$ $[M+H]^+$ 588.2547. Found 588.2549.

(2R,3S,5S)-5-(((((2S,3R)-2-amino-3-hydroxybutanamido)(hydroxy) phosphoryl)oxy)methyl)-2-(6-amino-9H-purin-9-yl)tetrahydrofuran-3-yl acetate (**4**). To a solution of intermediate **17** (39 mg, 0.066 mmol) in dry DCM (1 mL) TFA (0.51 mL, 6.64 mmol) was added at room temperature and the mixture was stirred for 1h. The volatiles were removed by evaporation *in vacuo*. The residue was treated with MeOH and the precipitate was collected by centrifugation to give product **4** (10 mg, 35% in two steps from **16**).^{1}H NMR (400 MHz, D_2O) δ 8.62 (s, 1H), 8.36 (s, 1H), 6.33 (d, J = 5.4 Hz, 1H), 4.85 – 4.77 (m, 1H), 4.49 – 4.39 (m, 1H), 4.23 (ddq, J = 11.7, 5.5, 2.7 Hz, 2H), 4.15 (ddd, J = 11.5, 6.4, 4.6 Hz, 1H), 3.94 (s, 1H), 2.49 (dt, J = 13.2, 6.6 Hz, 1H), 2.10 (ddd, J = 13.2, 9.2, 8.2 Hz, 1H), 1.29 (d, J = 6.5 Hz, 3H). ^{13}C NMR (400 MHz, D_2O) δ 169.74, 150.77, 148.20, 145.73, 143.03, 118.07, 85.63, 77.44, 70.86, 66.19, 65.83, 59.13, 31.93, 18.78. HRMS-ESI (m/z) calcd. for $C_{14}H_{23}N_7O_7P$ $[M+H]^+$ 486.1866. Found 486.1870.

In vitro PfThrRS inhibition assay

The bioassay protocol was adapted from literature.[18] The aminoacylation activity of PfThrRS in the presence of compounds was determined by measuring ATP consumption in the enzymatic reaction by using recombinant PfThrRS and *P. falciparum* cell extract as a source of t-RNA. ATP consumption was determined by Kinase-Glo® Reagent (Promega Inc.). The luminescence was read on a Tecan Infinite M1000 microplate reader. The inhibitory rate was measured in three independent assays. Borrelidin was obtained from commercial sources and used as a reference compound.

Expression and purification of PfThrRS and EcThrRS

Escherichia coli EcThrRS) was over-expressed in *E. coli* BL21(DE3) cells. Cells were grown in Luria-Bertani (LB) medium at 37 °C until OD_{600} = 0.8, when expression was induced with 0.5 mM IPTG for 16 h at 20 °C. *Plasmodium falciparum* PfThrRS was expressed in BL21(DE3) cells at 16 °C for 20 h using 0.5 mM IPTG. In both cases, cells were then harvested by centrifugation and resuspended in lysis buffer (20 mMTris pH 8.0, 300 mMNaCl, 1 mM TCEP and EDTA-free protease inhibitors). After sonication and ultracentrifugation, proteins were found predominantly in the soluble fraction. Both proteins were first purified by immobilized metal affinity chromatography (IMAC) with a 5 mL His-Trap column (GE Healthcare) and eluted with a linear imidazole gradient (0–0.5 M) in 15 column volumes (CV). The eluted fractions were then buffer-exchanged in 20 mM Tris pH 8.0, 1 mM TCEP, then loaded in a 5 mL ion exchange Q-

HP column (GE Healthcare) and eluted with a linear NaCl gradient (0–1 M) in 20 column volumes (CV). Selected fractions were then loaded in a Superdex 200 26/60 (Cytiva) in 20 mM Tris pH 8.0, 300 mM NaCl, and 1 mM TCEP and purified by size exclusion chromatography. No cleavage of the His-tag was done, and the yield was 7.5 mg/L (EcThrRS) and 2.0 mg/L (PfThrRS).

Isothermal titration calorimetry

Isothermal titration calorimetry (ITC) was used to determine the binding affinity between EcThrRS and ligand **4**. Experiments were performed on a MicroCal PEAQ-ITC (Malvern Panalytical) instrument. The ligand was diluted in the same buffer as the EcThrRS. Working ratio of EcThrRS and ligand was 20:200 µM. The method consisted of 20 sequential 2 µL injections, except the first injection whose volume was 0.4 µL. Time intervals between each injection was 150 seconds, stir speed 750 rpm, temperature in the cell 25 °C. Once the raw data was obtained, baseline and offset correction were performed. The first injection was excluded from the dataset. Finally, the processed experimental data was fitted to an independent model using MicroCal PEAQ-ITC Analysis Software v1.41.

Crystallization and X-ray structure determination

Crystallization experiments were done by the hanging drop method. Since PfThRS could not be crystallized, we used EcThRS to carry out structural analysis. To crystallize the EcThrRS –inhibitor **4** complex, the protein solution (10-15 mg/mL) was pre-mixed with 2 mM of compound **4** and incubated for 3 hr at 4 °C. The complex was then crystallized by mixing 1 µL of protein solution with 1 µL of a 12% (w/v) PEG 4000, 21% (v/v) MPD, and 0.1 M sodium citrate pH 5.9 crystallization buffer. Prior to X-ray diffraction data collection, crystals were flash-frozen in liquid nitrogen using 25% glycerol as cryoprotectant. Diffraction data were collected at the X06SA (PXI) beamline at the Swiss Light Source (SLS). Data were integrated and scaled within the DIALS suite[26]using XIA2.[27] The structures were determined by molecular replacement using the EcThrRS structure (PDB: 1NYQ) as the starting model and the program PHASER.[28] After corrections for bulk solvent and overall B values, data were refined by iterative cycles of positional refinement and TLS refinement with REFMAC[29] and model building with COOT[30] from the CCP4 suite.[31]Final coordinates have been deposited in the Protein Data bank (PDB accession code: 8OU8). Data collection and model statistics are shown in Table 1.

Table 1. Data collection and refinement statistics.

Wavelength	1.000
Resolution range	54.47 - 3.0 (3.107 - 3.0)
Space group	P 21 21 21
Unit cell	85.33 108.95 113.96 90 90 90
Total reflections	45827
Unique reflections	45827
Completeness (%)	99.79 (99.72)
CC 1/2	0.994 (0.747)
R-work	0.2730 (0.2942)
R-free	0.3300 (0.3720)
ligands	2
RMS(bonds)	0.0088
RMS(angles)	1.7600
Ramachandran favored (%)	92.36
Ramachandran allowed (%)	6.39
Ramachandran outliers (%)	1.25

Statistics for the highest-resolution shell are shown in parentheses.

Conclusions

A toxic moiety (TM84, **3a**) of the natural product Agrocin 84, known as an EcLeuRS inhibitor, was used as scaffold to design a threonine-containing analogue (**4**), which was then evaluated as malarial PfThrRS inhibitor. As we showed that analogue **4** displays submicromolar inhibitory potency against PfThrRS (IC_{50} = 440 nM), it complements the limited number of PfThrRS inhibitors known to date. We obtained the crystal structure of the *E. coli* homologue (EcThrRS) in complex with inhibitor **4** and we compared it to that of of EcLeuRS in complex with **3a** (TM84). The comparison revealed that the main differences are the presence of the zinc ion in the active site of ThrRS, which is involved in the recognition of the threonine moiety of inhibitor **4**. In addition, inhibitor **4** is located in the binding pocket of EcThrRS in a compact conformation that differs for the extended conformation of **3a** (TM84) in the pocket of the EcLeuRS. The structural differences between the binding of compounds **3a** and **4** to their host proteins involves different hydrogen bonding networks of the acylphosphoramidate, deoxyarabinose and adenosine moieties. These findings provide important structural information that can be used for the future design of novel ThrRS inhibitors e.g. based on acylphosphoramidate as a transition state mimic for aminoacylation reaction. Other future modifications could include bioisosteric replacement of adenine and deoxyarabinose part to achieve more drug-like ThrRS inhibitors.

Conflicts of interest

There are no conflicts to declare.

Acknowledgements

The work has been funded by European Regional Development Fund (Agreement Nr. 1.1.1.1/19/A/019).

Notes and references

1. *WHO, World Malar. Rep. 2022 World Health Organ. Geneva 2016 https://www.who.int/publications/i/item/9789240064898*
2. J. E. Hyde, *The FEBS Journal*, 2007, **274**, 4688-4698.

3. T. N. Wells, P. L. Alonso and W. E. Gutteridge, *Nature Rev. Drug Disc.*, 2009, **8**, 879-891.
4. V. Rajendran, P. Kalita, H. Shukla, A. Kumar and T. Tripathi, *Int. J. Biol. Macromol.*, 2018, **111**, 400-414.
5. G. H. Vondenhoff and A. Van Aerschot, *Eur. J. Med. Chem.*, 2011, **46**, 5227-5236.
6. N. H. Kwon, P. L. Fox and S. Kim, *Nature Rev. Drug Disc.*, 2019, **18**, 629-650.
7. L. Pang, S. D. Weeks and A. Van Aerschot, *Int. J. Mol. Sci.*, 2021, **22**, 1750.
8. C. S. Francklyn and P. Mullen, *J.Biol. Chem.,* 2019, **294**, 5365-5385.
9. S.-H. Kim, S. Bae and M. Song, *Biomolecules,*2020, **10**, 1625.
10. G. Bouz and J. Zitko, *Bioorg. Chem.*, 2021, **110**, 104806.
11. C. S. Francklyn and P. Mullen, *J. Biol. Chem.*, 2019, **294**, 5365-5385.
12. P. Fang, X. Yu, S. J. Jeong, A. Mirando, K. Chen, X. Chen, S. Kim, C. S. Francklyn and M. Guo, *Nature Comm.*, 2015, **6**, 6402.
13. A. Saint-Léger, C. Sinadinos and L. Ribas de Pouplana, *Bioengineered*, 2016, **7**, 60-64.
14. D. W. Nyamai and Ö. Tastan Bishop, *Malaria J.* 2019, **18**, 34.
15. K. Otoguro, H. Ui, A. Ishiyama, M. Kobayashi, H. Togashi, Y. Takahashi, R. Masuma, H. Tanaka, H. Tomoda, H. Yamada and S. Omura, *J. Antibiot.*, 2003, **56**, 727-729.
16. A. Sugawara, T. Tanaka, T. Hirose, A. Ishiyama, M. Iwatsuki, Y. Takahashi, K. Otoguro, S. Ōmura and T. Sunazuka, *Bioorg. Med. Chem. Lett.*, 2013, **23**, 2302-2305.
17. E. M. Novoa, N. Camacho, . M. Bautista, A. C. Mirando, C. S. Francklyn, S. Varon, M. Royo, A. Cortes and L. Ribas de Pouplana, *PNAS*, 2014, **111**, E5508-5517.
18. J. Guo, B. Chen, Y. Yu, B. Cheng, Y. Ju, J. Tang, Z. Cai, Q. Gu, J. Xu and H. Zhou, *Eur. J. Med. Chem.*, 2020, **207**, 112848.
19. M. Teng, M. T. Hilgers, M. L. Cunningham, A. Borchardt, J. B. Locke, S. Abraham, G. Haley, B. P. Kwan, C. Hall, G. W. Hough, K. J. Shaw and J. Finn, *J.Med.Chem.*, 2013, **56**, 1748-1760.
20. Z. Cai, B. Chen, Y. Yu, J. Guo, Z. Luo, B. Cheng, J. Xu, Q. Gu and H. Zhou, *J.Med.Chem*, 2022, **65**, 5800-5820.
21. H. Qiao, M. Xia, Y. Cheng, J. Zhou, L. Zheng, W. Li, J. Wang and P. Fang, *Communications Biology*, 2023, **6**, 107.
22. J. Guo, B. Chen, Y. Yu, B. Cheng, Y. Cheng, Y. Ju, Q. Gu, J. Xu and H. Zhou, *Eur. J. Med. Chem.*, 2020, **187**, 111941.
23. S. Chopra, A. Palencia, C. Virus, A. Tripathy, B. R. Temple, A. Velazquez-Campoy, S. Cusack and J. S. Reader, *Nat. Commun.*, 2013, **4**, 1417.
24. D. Y. Travin, K. Severinov and S. Dubiley, *RSC Chem.Biol.* 2021, **2**, 468-485.
25. M. Kawana, M. Nishikawa, N. Yamasaki and H. Kuzuhara, *J. Chem. Soc., Perkin Trans1*, 1989, 1593-1596.
26. G. Winter, J. Beilsten-Edmands, N. Devenish, M. Gerstel, R. J. Gildea, D. McDonagh, E. Pascal, D. G. Waterman, B. H. Williams and G. Evans, *Protein Sci*, 2022, **31**, 232-250.
27. R. J. Gildea, J. Beilsten-Edmands, D. Axford, S. Horrell, P. Aller, J. Sandy, J. Sanchez-Weatherby, C. D. Owen, P. Lukacik, C. Strain-Damerell, R. L. Owen, M. A. Walsh and G. Winter, *Acta Crystallogr. Sect. D*, 2022, **78**, 752-769.
28. A. J. McCoy, R. W. Grosse-Kunstleve, P. D. Adams, M. D. Winn, L. C. Storoni and R. J. Read, *J. Appl. Crystallogr.*, 2007, **40**, 658-674.
29. A. A. Vagin, R. A. Steiner, A. A. Lebedev, L. Potterton, S. McNicholas, F. Long and G. N. Murshudov, *Acta Crystallogr. D.,*2004, **60**, 2184-2195.
30. P. Emsley and K. Cowtan, *Acta Crystallogr. D.,* 2004, **60**, 2126-2132.
31. M. D. Winn, C. C. Ballard, K. D. Cowtan, E. J. Dodson, P. Emsley, P. R. Evans, R. M. Keegan, E. B. Krissinel, A. G. Leslie, A. McCoy, S. J. McNicholas, G. N. Murshudov, N. S. Pannu, E. A. Potterton, H. R. Powell, R. J. Read, A. Vagin and K. S. Wilson, *Acta Crystallogr. D.,* 2011, **67**, 235-242.